



HAL
open science

Tethered Counterion-Directed Catalysis: Merging the Chiral Ion-pairing and Bifunctional Ligand Strategies in Enantioselective Gold(I) Catalysis

Zhenhao Zhang, Vitalii Smal, Pascal Retailleau, Arnaud Voituriez, Gilles Frison, Angela Marinetti, Xavier Guinchard

► **To cite this version:**

Zhenhao Zhang, Vitalii Smal, Pascal Retailleau, Arnaud Voituriez, Gilles Frison, et al.. Tethered Counterion-Directed Catalysis: Merging the Chiral Ion-pairing and Bifunctional Ligand Strategies in Enantioselective Gold(I) Catalysis. *Journal of the American Chemical Society*, 2020, 142, pp.3797-3805. 10.1021/jacs.9b11154 . hal-02471058

HAL Id: hal-02471058

<https://hal.science/hal-02471058>

Submitted on 7 Feb 2020

HAL is a multi-disciplinary open access archive for the deposit and dissemination of scientific research documents, whether they are published or not. The documents may come from teaching and research institutions in France or abroad, or from public or private research centers.

L'archive ouverte pluridisciplinaire **HAL**, est destinée au dépôt et à la diffusion de documents scientifiques de niveau recherche, publiés ou non, émanant des établissements d'enseignement et de recherche français ou étrangers, des laboratoires publics ou privés.

Tethered Counterion-Directed Catalysis: Merging the Chiral Ion-pairing and Bifunctional Ligand Strategies in Enantioselective Gold(I) Catalysis

Zhenhao Zhang,^{a,b} Vitalii Smal,^a Pascal Retailleau,^a Arnaud Voituriez,^a Gilles Frison,^b Angela Marinetti,^{*a} Xavier Guinchard^{*a}

^a Institut de Chimie des Substances Naturelles, CNRS UPR 2301, Université Paris-Sud, Université Paris-Saclay, 1 avenue de la Terrasse, 91198 Gif-sur-Yvette, France.

^b LCM, CNRS, Ecole Polytechnique, Institut Polytechnique de Paris, 91128 Palaiseau, France.

Supporting Information Placeholder

ABSTRACT: Tethering a metal complex to its phosphate counterion via a phosphine ligand enables a new strategy in Asymmetric Counterion-Directed Catalysis (ACDC). A straightforward, scalable synthetic route gives access to the gold(I) complex of a chiral phosphine displaying a phosphoric acid function. The complex generates a catalytically active species with an unprecedented intramolecular relationship between the cationic Au(I) center and the phosphate counterion. The benefits of tethering the two functions of the catalyst is demonstrated here in a tandem cycloisomerization/nucleophilic addition reaction, by attaining high enantioselectivity levels (up to 97% ee) at a remarkable low 0.2 mol% catalyst loading. Remarkably the method is also compatible with a silver-free protocol.

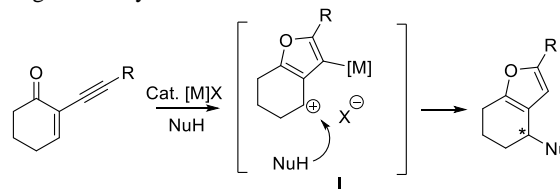
INTRODUCTION

The challenge of enantioselective gold(I) catalysis clearly relates to the linear geometry of the active complexes as well as, in many instances, to the outer-sphere mechanisms of the enantiodetermining step. Nevertheless, high enantioselectivity could be achieved in recent years by means of either sterically congested ligands, which create deep chiral pockets embedding the distal active site, bifunctional phosphines or by dinuclear complexes possibly shaped through aurophilic interactions.¹ Alternatively, Toste² introduced the chiral counterion strategy, where notably BINOL-derived phosphates operate as chiral inducers in reactions involving cationic gold intermediates. Despite some uncertainties over the exact mechanisms and role of the phosphate anions, this strategy has shown prominent potential and has triggered significant advances in both gold^{3,4} and other transition metal catalysis.^{5,6} In gold(I) catalysis, the first disclosed intramolecular hydroalkoxylation, hydrocarboxylation and hydroamination reactions remain so far the main application domains of the counterion strategy, although the method should apply, in theory, to a much wider range of reactions. Notably all reactions involving tight ion pairs in the enantiodetermining step are potentially suitable, including those going through carbocationic intermediates with remote, neutral gold(I) units. This scenario is suitably typified by the tandem heterocyclization-nucleophilic addition reactions in Scheme 1.1.⁷ In this case and others, the stereochemical control from the chiral counterion suffers however from the poorly defined and flexible spatial arrangement of the phosphate-carbocation pair. We suggest that this drawback might be overcome by tethering somehow the phosphate counterion to the cationic Au complex (Scheme 1.2b). A covalent tether connecting the phosphate unit to a gold ligand might afford sufficient geometrical constraints and molecular organization to the key intermediate to allow efficient stereochemical control. This approach, when properly implemented, might push the limits of the ‘ion-pairing strategy’ in enantioselective gold catalysis and, more broadly, in enantioselective transition metal catalysis. Previous transition metal complexes embedding intramolecularly an anion have been reported. However in these

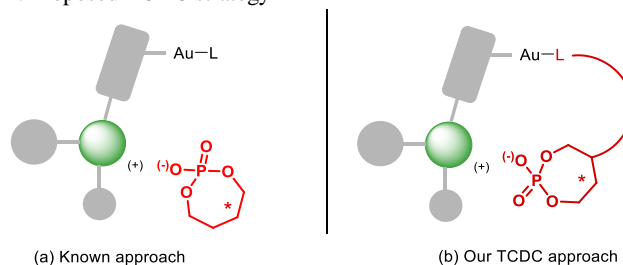
cases, the chiral ligand does not dissociate from the metal all throughout the catalytic process.⁸

Scheme 1. Proposed Enhanced Strategy for Asymmetric Ion-pair Catalysis: Tethering a Chiral Phosphate Unit to the Metal Complex.

1. Targeted catalytic reactions



2. Proposed TCDC strategy



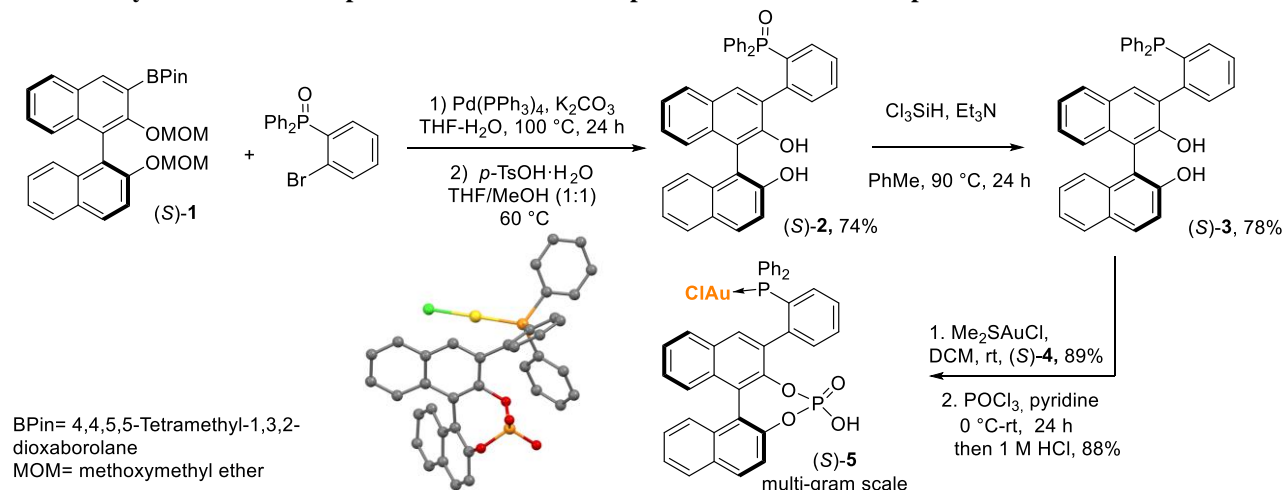
In this paper, we report on the specific design of a new bifunctional ligand⁹ combining a mono-phosphine and a remote BINOL-derived phosphate function. As a proof of concept, we show that the corresponding Au(I) complex¹⁰ gives so far unattained levels of enantioselectivity in the cycloisomerization/addition sequence depicted in Scheme 1.1, at very low catalytic loading. Theoretical studies enlighten and support mechanistic hypotheses on the role of the phosphate counterion in these reactions.

RESULTS AND DISCUSSION

The targeted Au-precatalyst (*S*)-**5** contains an (*S*)-BINOL-derived phosphoric acid moiety, with an *ortho*-(diphenylphosphino)phenyl

substituent at its 3-position.^{11,8a} The key steps for the synthesis of the LAuCl complex (*S*)-5, shown in Scheme 2, were inspired

Scheme 2. Synthesis of the Phosphoric Acid-tethered Phosphine Gold Chloride Complex 5



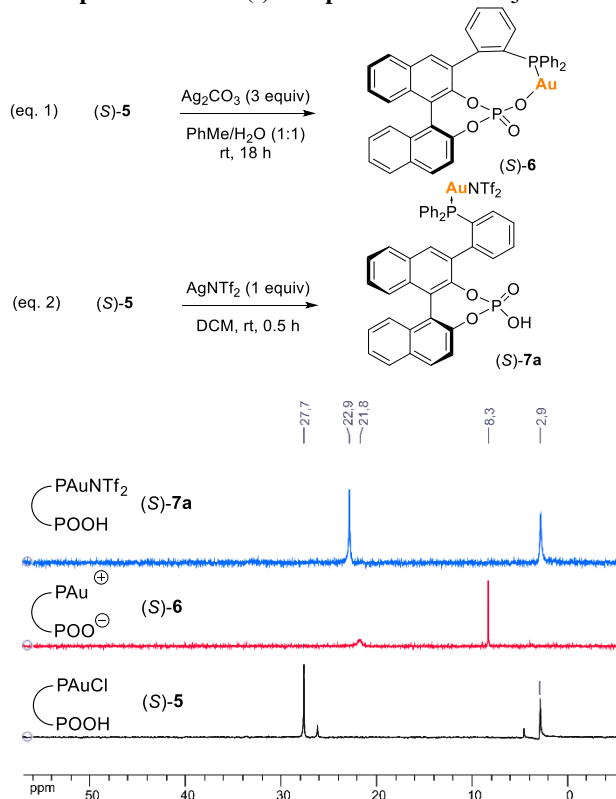
by the respective work of Iwa and Sawamura,^{8a} and Sasai¹² who reported on the synthesis of BINOL-based bifunctional phosphines and studied their rhodium coordination or applications in organocatalysis, respectively.

The synthetic approach starts with the synthesis of the BINOL-substituted triarylphosphine oxide (*S*)-2¹²⁻¹³ via the palladium coupling of boronate (*S*)-1¹⁴ with (2-bromophenyl)diphenylphosphine oxide, followed by MOM group removal in acidic conditions. The phosphine oxide (*S*)-2 is obtained in an overall 74% yield. Reduction with chlorosilane gives then the trivalent phosphine (*S*)-3 that displays two sets of signals in both ³¹P and ¹H NMR spectra, as reported previously (³¹P NMR $\delta = -10.6$ and -12.3 ppm). Complexation of (*S*)-3 to Au(I) was carried out successfully using Me₂SAuCl as the starting material. The final setup of the cyclic phosphoric acid unit was done via a classical procedure, by using P(O)Cl₃ as the phosphorylating agent followed by an acidic hydrolysis. It afforded the desired (phosphine)AuCl complex (*S*)-5 as a crystalline solid in 88% isolated yield.¹⁵ The whole sequence could be scaled-up to several grams without notable difficulties (3.15 g of (*S*)-5 has been isolated, 3.7 mmol). The molecular structure of (*S*)-5 has been ascertained by X-ray crystallography (Scheme 2). The ³¹P NMR spectrum of acid (*S*)-5 in CDCl₃ shows a 4:1 mixture of two species (³¹P NMR in CDCl₃: $\delta = 27.6$ and 2.9 ppm for the major isomer; $\delta = 26.2$ and 4.6 ppm for the minor isomer, see Figure 1a), tentatively assigned as equilibrating rotamers. When the ³¹P NMR of compound (*S*)-5 was recorded in deuterated pyridine, very clean spectra were obtained showing a single set of signals (³¹P NMR in *d*₅-Pyridine: $\delta = 29.2$ and 6.7 ppm). In *d*₆-DMSO at room temperature, compound (*S*)-5 also displays two sets of broad signals, which coalesce into a single set at 110 °C ($\delta = 26.8$ ppm and 1.1 ppm).

Chloride abstraction from the gold complex (*S*)-5 has been carried out then with the basic silver carbonate, so as to also deprotonate concomitantly the phosphoric acid function (Scheme 3, eq. 1). From this experiment, the putative Au(I) complex (*S*)-6 was obtained. Its ³¹P NMR spectrum shows a broad signal at $\delta = 21.8$ ppm and a sharp one at 8.4 ppm. These data are in agreement with the postulated formation of the phosphine-phosphate complex, since both phosphorus signals are significantly shifted with respect to (*S*)-5. Structurally related gold(I) phosphates from the

literature also display ³¹P NMR chemical shifts in the range 8-10 ppm, in CD₂Cl₂.¹⁷ Interestingly, complex 6 do not show ³¹P-³¹P coupling in ³¹P NMR, indicating that the gold-oxygen interaction may be more ionic than covalent.¹⁸

Scheme 3. Conversion of (*S*)-5 to cationic Au(I) species and ³¹P NMR Spectra of the Au(I) Complexes 5-7 in CDCl₃



The molecular formula of (*S*)-6 has been ascertained by mass spectrometry (ESI *m/z* calculated for [M+HCOO]⁺ = 849.0781; found: *m/z* = 849.0876). For comparison purposes, complex (*S*)-5 was reacted also with AgNTf₂, to give a new complex (*S*)-7a. The ³¹P NMR of (*S*)-7a was diagnostic for a Cl/NTf₂ exchange (high-field shift of the phosphine signal from 27.7 to 22.9 ppm), while

the signal of the phosphoric acid group remained unchanged at 2.9 ppm. Overall, although we could not obtain so far crystals of (*S*)-**6** suitable for X-ray diffraction studies, both mass spectrometry and NMR data tend to support the structural assignment, although they can't discriminate so far between monomeric species and more complex assemblies in solution. Assemblies would have however little incidence on catalytic processes, since coordination of the substrates will generate then the same active species.

We then turned straight to catalytic tests by investigating the tandem cycloisomerization/nucleophilic additions of 2-alkynyl-enones typified in Table 1. As pointed out above, the rationale behind this choice is that these reactions should involve carbocation-phosphate pairs as the key intermediates and therefore benefit from tethering gold to the chiral phosphate. The reaction, initially reported by Larock⁷ by using AuCl₃ as the catalyst, leads to synthetically relevant, highly substituted furans. It applies to a number of 2-alkynyl-enones (cyclohexenones, chromones, acyclic enones) and tolerates a large set of nucleophilic partners: alcohols, water, 1,3-dicarbonyls, indoles, allenamides, anilines and carbamates. With imines,¹⁹ allenamides,²⁰ 3-styrylindoles²¹ and nitrones²² as the nucleophiles, 3,4-fused bicyclic furans are obtained. Beside Au(III) and Au(I) catalysts,²³ also Pt(II),²⁴ Pd(II),²⁵ Ag(I),²⁶ Cu(I), Cu(II),²⁷ and In(III)²⁸ salts proved to be good catalysts. Despite the wide synthetic potential of these reactions, enantioselective variants have been implemented successfully for only a few substrate pairs. Beyond Toste's initial report on indole nucleophiles (Cu(TRIP)₂ catalysts)^{27b} and our recent report with Ag⁺ catalysts,²⁶ notable examples are the reactions carried out with nitrones,^{9a, 29} 3-styrylindoles²¹ and allenamides²⁰ using either bis-gold complexes of diphosphines or mono-gold complexes of sulfonamide-functionalized phosphines and phosphoramidites.

The gold complex (*S*)-**5** was evaluated initially in the reaction of 2-(phenylethynyl)-2-cyclohexenone **8a** with indole **9a**. Comparative experiments were also performed to support the postulated involvement of the phosphate function in the stereochemical control of this reaction. Selected experiments are reported in Table 1. Initial experiments showed that *in situ* activation of (*S*)-**5** with Ag₂CO₃ in various solvents, enables a good catalytic activity, with up to 88% ee for reactions performed in toluene (Table 1, entries 2-4).³⁰ Most rewardingly, the precatalyst loading could be gradually decreased from 5 to 2, 0.2, 0.1 and 0.05 mol% leading to constantly good yields and enantioselectivities (91-96% ee, entries 4-9). In the context of enantioselective Au(I) catalysis, where a 3-5 mol% catalyst loading is usually employed, a 0.05 mol% catalyst loading is extremely low. This excellent catalytic activity (TON 1400) might suggest an exceptional stability of the resting state of the catalyst towards decay, possibly due to the tight intramolecular pairing between Au(I) and its phosphate counterion. Alternatively, the high reactivity might be assigned to the strained, non-linear coordination of gold in complex **6** (see calculated geometries hereafter), which would decrease the deformation energy required for the coordination of the substrate.³¹

A few experiments have been carried out then, whose results overall confirm the role of the phosphate tether.

- Catalysts (*S*)-**7a,b**, generated from (*S*)-**5** with the non-basic silver salts AgNTf₂ and AgSbF₆, gave significantly lower enantiomeric excesses (entries 10, 11).

- Catalysts (*S*)-**11a,b** which display the same molecular scaffold as (*S*)-**5** but a methyl phosphate function, instead of the phosphoric acid function, give very low enantiomeric excesses.³²

- The (Ph₃P)Au(TRIP) complex (*R*)-**12**, that may be viewed as a non-chelated structural analogue of **6**, gives a much lower enantiomeric excess (24% ee,²⁶ entry 14).

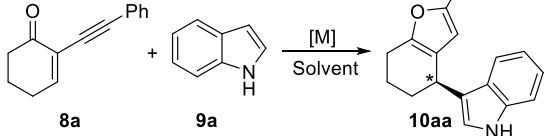
- Another non-chelated analogue has been prepared purposely: the (Ph₃P)Au(phosphate) (*S*)-**13a** which contain the same tethered phosphine/phosphate of (*S*)-**5** but displays an oxidized phosphorus function. It gave a racemic product (entry 15).

Finally, from results in Table 1, it may be noted that Ag₂CO₃ does not catalyze, by itself, this reaction (entry 1) and the silver phosphate (*S*)-**13b** displays low catalytic activity and low enantioselectivity (entry 16). Therefore, silver catalysis should not compete significantly with the gold promoted catalytic process in entries 4-9.

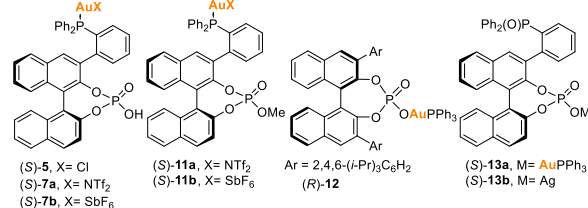
The absolute configuration of the final product **10aa** has been established, for the first time in this series, by X-ray crystallography (see Supporting Information). The (*S*)-configured catalyst **5** gives (*R*)-**10aa** as the major enantiomer.

Overall, the comparative experiments in Table 1 clearly highlight the positive effect of tethering the phosphine and phosphate functions and therefore substantiate our catalyst design and working hypothesis.

Table 1. Enantioselective Cyclization/Indole Addition Reactions: Optimization with Precatalyst (*S*)-5**^a**



entry	cat. (mol%)	additive (mol%)	solvent	yield (%) ^b	ee ^c (%)
1	-	Ag ₂ CO ₃ (5)	PhMe	0	-
2	(<i>S</i>)- 5 (5)	Ag ₂ CO ₃ (2.5)	MeCN	76	12
3	(<i>S</i>)- 5 (5)	Ag ₂ CO ₃ (2.5)	THF	29	86
4	(<i>S</i>)- 5 (5)	Ag ₂ CO ₃ (2.5)	PhMe	69	88
5	(<i>S</i>)- 5 (2)	Ag ₂ CO ₃ (1)	PhMe	88	91
6	(<i>S</i>)- 5 (0.2)	Ag ₂ CO ₃ (0.1)	PhMe	75	96
7	(<i>S</i>)- 5 (0.2)	Ag ₂ CO ₃ (1)	PhMe	68	94
8	(<i>S</i>)- 5 (0.1)	Ag ₂ CO ₃ ^d	PhMe	73	93
9	(<i>S</i>)- 5 (0.05)	Ag ₂ CO ₃ ^d	PhMe	70	91
10	(<i>S</i>)- 7a (0.2)	-	PhMe	85	29
11	(<i>S</i>)- 7b (0.2)	-	PhMe	76	62
12	(<i>S</i>)- 11a (0.2)	-	PhMe	85	15
13	(<i>S</i>)- 11b (0.2)	-	PhMe	90	12
14	(<i>R</i>)- 12 (10)	-	PhMe	60	24 ²⁶
15	(<i>S</i>)- 13a (0.2)	-	PhMe	70	0
16	(<i>S</i>)- 13b (0.2)	-	PhMe	12	10



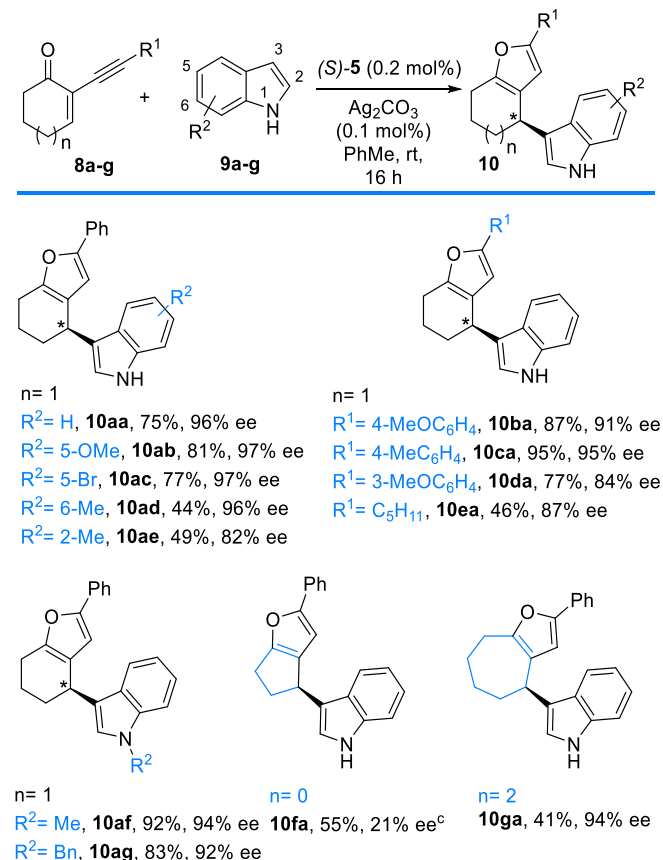
^a Reactions were run with a 1:1 ratio of **8a** and **9a**, at rt for 18 h. Reactions in entries 1-5 were performed at a 0.1 mmol scale (0.1 M). In entries 6-10 (0.55 mmol scale), the concentration of the catalyst was 0.4 mM. ^b Isolated yields. ^c Determined by chiral HPLC. ^d At low catalytic loading, the silver carbonate was used in excess, with no impact on the enantioselectivity level.

The high catalytic performance of (*S*)-**5** in the reaction above, encouraged us then to investigate the substrate scope by considering the substituted indoles **9b-g** (Scheme 4). Substituents such as methoxy-, bromine, and methyl groups were tolerated on the C5 and C6 positions of indole delivering **10ab-ad** in high enantiomeric excesses. Interestingly, the C2-substituted 2-methylindole gave **10ae** in high ee and higher yield than the Cu(II) based method.^{27b}

In a second series of experiments, the 2-alkynyl-cyclohexenones **8b-e**, displaying various R¹ groups, were reacted with indole **9a** (R²=H). For R¹ = *p*-anisyl, *p*-tolyl, and *m*-anisyl, the corresponding bicyclic furanes **10ba**, **10ca** and **10da** were obtained in high yields and enantioselectivities. Finally, an alkyl substituted substrate **8e** (R¹ = C₅H₁₁) was reacted with indole and led to the expected furane **10ea** with 87% ee.

Most notably, the reaction between *N*-Me-indole **9f** and **8a** delivered the addition product **10af** in high yield (92%) and enantiomeric excess (94% ee). A similar level of enantioselectivity was then obtained from *N*-benzyl indole **9g** (**10ag**, 92%). These two results are crucial to enlighten the mechanism of the stereochemical control. They indeed indicate that the NH function of indole is not essential and rule out the involvement of H-bonds between phosphate and indole in the stereodetermining step. They also demonstrate that our method enables the previously unsuccessful use of *N*-substituted indoles in these catalytic reaction.²⁶ Cyclopentenone **8f** and cycloheptanone **8g** were then used in the reaction leading to the corresponding bicyclic furanes **10fa** and **10ga** in 21% ee and 94% ee, respectively. These unprecedented reactions show that the enantioselective cyclization/nucleophilic addition sequence apply successfully, not only to six-membered but also to seven-membered enones.

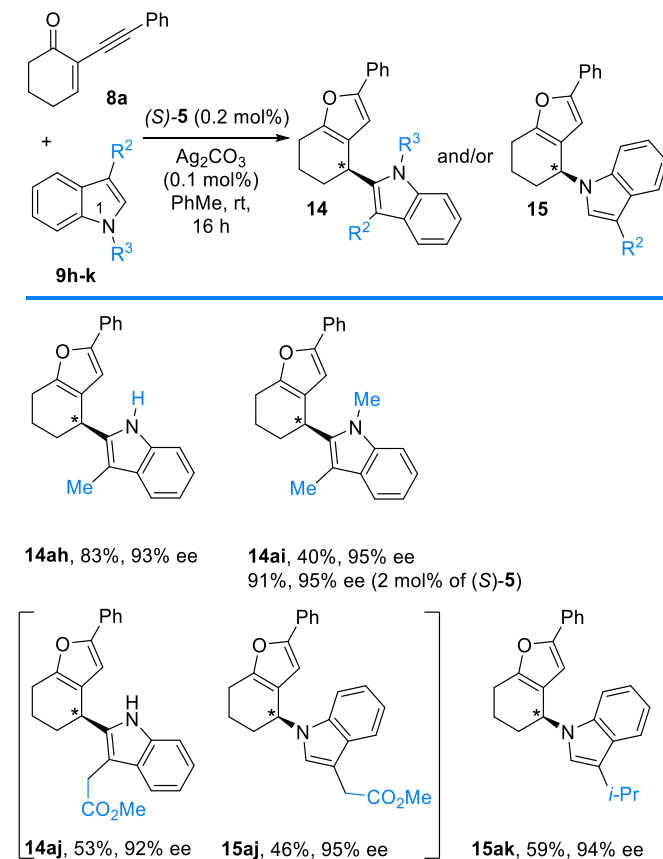
Scheme 4. Scope of the Enantioselective Addition of Indoles **9** to Enones **8**.



^a Isolated yields. ^b Enantiomeric excesses were determined by chiral HPLC. ^c Reaction performed with 2 mol% of the precatalyst **5**.

In another series of experiments, 3-substituted indoles were considered (Scheme 5). 3-Methylindole could be reacted: addition through its C2-position afforded compound **14ah** in high yield and enantioselectivity (93% ee). Extension of the process to 1,3-dimethylindole gave **14ai** in high 95% ee but moderate yield, that could however be increased to 91% using 2 mol% of the catalyst. When increasing the steric hindrance at the C3 position we observed, interestingly, that the reaction leads to mixtures of two products resulting from C2 and *N*-alkylations, respectively. While methyl-3-indolylacetate **9j** led to an essentially 50/50 mixture of **14aj** and **15aj** in excellent ee's, the 3-isopropylindole **9k** afforded mainly the *N*-alkylated product **15ak** in 94% ee. This unusual behavior offers the possibility to engage the three potentially nucleophilic positions of indoles in highly enantioselective cyclization/addition of indoles processes.

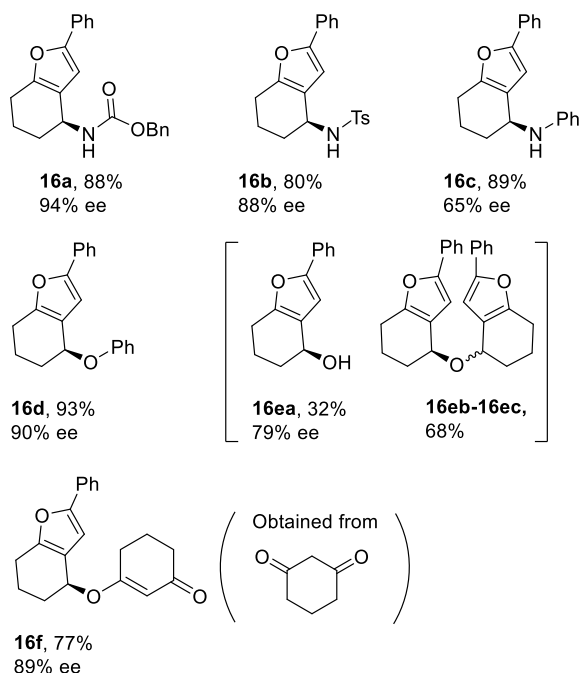
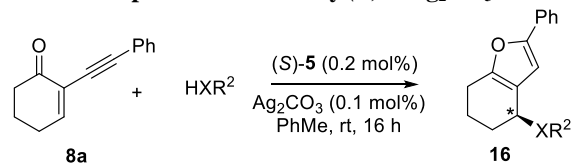
Scheme 5. Enantioselective Additions of C3-substituted Indoles to Enone **8a**.



The *N*-additions observed here encouraged us to move then to totally different series of nucleophiles as reaction partners. We were pleased to find that unprecedented enantioselectivity levels can be attained with hetero-nucleophiles such as benzylcarbamate (94% ee), tosylamide (87% ee) and phenol (90% ee) (Scheme 6). Noteworthy, even the simple addition of water takes place with

high stereocontrol, leading to the alcohol **16ea** in 79% ee. The reaction also affords ethers **16eb** and **16ec** (homochiral **16eb** 50% yield, *meso* **16ec** 18% yield). Finally, the use of cyclohexanedione as nucleophile afforded **16f** in 77% yield and 89% ee, resulting from O-addition of the nucleophile to the carbocation, as previously observed by Larock.^{7b} Overall these experiments demonstrate the high stereocontrol induced by the newly designed (*S*)-**5**/Ag₂CO₃ catalytic system in reactions involving a variety of nucleophiles from substituted indoles to simple nitrogen and oxygen nucleophiles.

Scheme 6. Enantioselective Tandem Cyclisation - Addition of Heteronucleophiles Promoted by (*S*)-**5**/Ag₂CO₃



Finally, during these studies, we disclosed rewardingly that activation of precatalyst (*S*)-**5** by a silver salt may not be systematically required (Table 2). The reaction of ketones **8a** and **8g** with representative nucleophiles could be performed in the presence of (*S*)-**5** only and the corresponding products were obtained in moderate to good yields and very high enantiomeric excesses. The gold chloride (*S*)-**5** gives a slightly lower reaction rate, with respect to the Ag₂CO₃ activated catalyst. Thus, we believe that the precatalyst reacts in situ with the weakly basic nucleophiles of the reaction mixture, resulting in the spontaneous, reversible formation of the active gold phosphate catalyst by HCl abstraction. The precatalyst **5** may thus be considered as a reservoir of stable Au(I) complex gradually delivering the active catalyst. This rare property of (*S*)-**5** may be extremely important in the general context of Au(I) catalysis, where the effects of silver salts are far from being benign.^{4b, 33}

Table 2. Use of Non-activated (*S*)-5** in the Enantioselective Cyclization/Addition Reactions:**

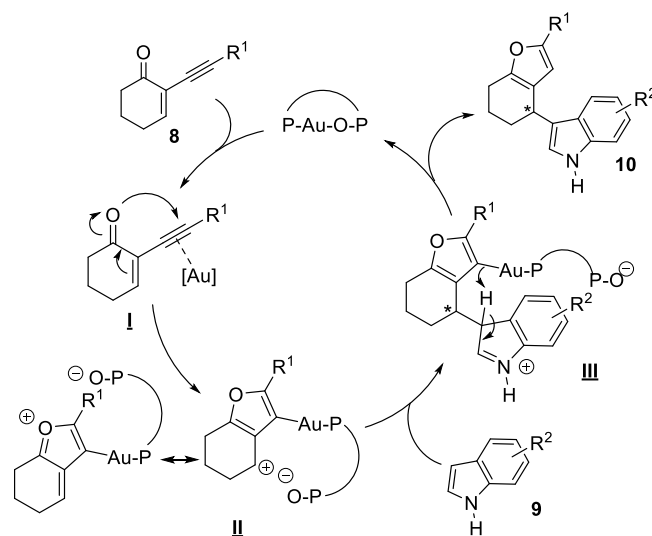
entry	8	nucleophile	product	yield (%) ^a	ee (%) ^b
1	8a	9a	10aa	80	92
2	8a	9b	10ab	73	94
3	8a	9c	10ac	30	75
4	8g	9a	10ga	55	95
5	8a	TsNH ₂	16b	41	88

^a Isolated yields. ^b Determined by chiral HPLC.

The search for alternative silver-free gold catalysts is a long-lasting quest.³⁴ Most approaches rely on protic acid activation of LAuMe complexes,³⁵ Brønsted acid activation of LAu(OH),³⁶ activation of LAuCl with silylium³⁷ or Cu(OTf)₂,³⁸ and addition of a Brønsted acid/Lewis acid to (PPh₃)Au(Ph).^{33c} As far as we know, a spontaneous dissociation of an IPrAuCl Au(I) complex has been claimed only in the gold-catalyzed hydration of alkynes.³⁹

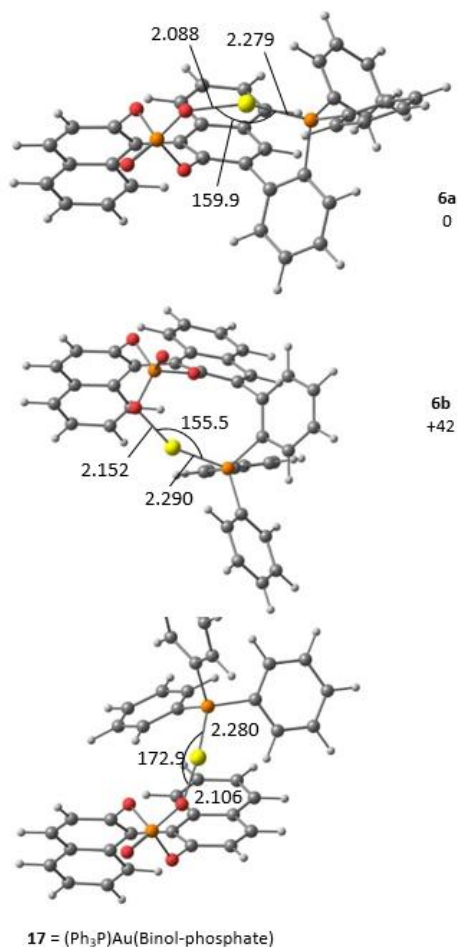
The mechanistic pathway currently postulated for these reactions is illustrated in Scheme 7, with enone **8** and indole **9** as the substrates. Activation of the alkyne unit by Au(I) (Int. **I**) triggers the cycloisomerization of enone **8** into the cationic intermediate **II** featuring a phosphate counterion. The nucleophilic addition of indole to **II**, leads then to intermediate **III**. From **III**, the proto-deauration step proceeds through formal H-transfer, that might be mediated actually by the phosphate itself, or by trace amounts of other bases (e.g. HO⁻). According to the postulated mechanism below, high enantioselectivity levels should result from a tight ion pairing in intermediate **II** which will bring the chiral phosphate unit closer to the prochiral carbon in the enantiodetermining step. It can be assumed that the geometrical constraints enforced by tethering gold(I) to phosphate, create a more organized spatial arrangement in **II** and enable the excellent stereocontrol.

Scheme 7. Postulated Mechanistic Pathway



To gain better insight into the structure of the potential catalyst (*S*)-**6** and the postulated reaction intermediates **II** and **III**, we have carried out computational studies at the DFT level (see the SI for computational details). The lowest energy structure for monomeric catalyst (*S*)-**6** is displayed in Figure 1 (**6a**). It shows that coordination of the phosphate to gold involves preferentially the *pro-S* oxygen atom, which gives a *S*-configured phosphorus. Coordination of the other PO unit would lead to **6b** which is 42 kJ.mol⁻¹ higher in energy compared to **6a**, due to its more distorted and strained geometry (P-Au-O bond angle = 155.5° for **6b** vs 159.9° for **6a**; Au-P = 2.290 Å for **6b** vs 2.088 Å for **6a**).

Figure 1. DFT Calculated Structures of Catalyst (*S*)-6** and its Non-tethered Analogue **17**. Relative Gibbs Free Energy in kJ.mol⁻¹.**

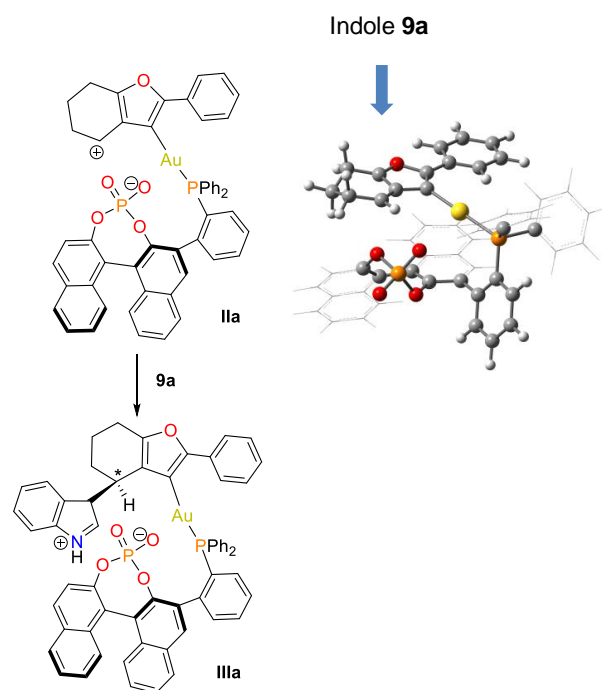


Examination of the metrical parameters of **6a** around the metal center reveals a significantly bent phosphine-gold-phosphate unit (P-Au-O bond angle = 159.9°), due to the geometrical constraints enforced by the molecular backbone of the ligand. For comparison, the geometry of the non-tethered (triphenylphosphine)gold(I) BINOL-phosphate complex **17** has been calculated as well (Figure 1). In **17**, the linearity at gold is almost restored (P-Au-O bond angle = 172.9°), in line with the previously reported X-ray structure (172.7°).¹⁷ The deviation from linearity observed in **6** has only limited effect on the bond lengths: the Au-P (2.279 Å) and Au-O (2.088 Å) bond distances are similar to those observed

experimentally for a (triphenylphosphine)gold-phosphate (2.20 and 2.058 Å respectively)¹⁷ and its computational model **17** (2.280 and 2.106 Å respectively). The bent geometry of the complex might have effects on the energy profile throughout the catalytic cycle.

The key carbocationic intermediate **IIa** features an electrostatic pairing between the carbocation and the tethered phosphate group leading to the preferred conformation shown in Figure 2. The stereochemistry control should result then from two combined effects: the preferred conformation of the zwitterionic intermediate **IIa** and the preferred addition of the nucleophilic indole that is likely to take place from the face opposite to the phosphate group. Importantly, the resulting configuration of stereogenic center in **IIIa** converges with that of the final product **10a** established by X-Ray crystallography (*R*-configuration). Overall, our preliminary calculations (See Supporting Information) highlight (a) the non-linear geometry of the P-Au-O moiety in catalyst **6** that might be responsible for its increased reactivity; (b) an easy cycloisomerization process triggered by gold(I) ($\Delta G^\ddagger = 36.6$ kJ.mol⁻¹); (c) the strong preference of the carbocationic intermediate **II** for ion-pairing with the phosphate anion; (d) an exoergonic nucleophilic addition step taking place from the less hindered face, opposite to the phosphate group.

Figure 2. Optimized Geometry of Intermediate IIa and Postulated Direction of the Nucleophilic Addition (for clarity, a wireframe representation of some aryl groups is used).



CONCLUSION

In conclusion, this work affords clear evidence that tethering of a phosphine and a phosphoric acid functions, represents a promising new approach to catalysts design. By combining the chiral counterion strategy and the remote cooperative group strategy, this design has enabled unprecedented enantioselectivity levels to be attained in a highly synthetically useful reaction. Tethering of the phosphate counterion also produces a rare example of gold chlo-

ride complex that do not require activation by silver salts. While in gold catalysis the ACDC strategy was hitherto limited to intramolecular processes the counterion tethering approach allowed us to successfully develop an intermolecular reaction. Following to this proof of concept, the Tethered Counterion-Directed Catalysis (TCDC) should find applications not only in a range of gold(I) catalyzed reactions, but also in a number of processes promoted by other transition metals. The scope of these catalysts is being investigated in our group.

ASSOCIATED CONTENT

Supporting Information

The Supporting Information is available free of charge on the ACS Publications website. Details of the experimental procedures, NMR spectra, HPLC data and computational data (pdf), CIF files (.cif)

AUTHOR INFORMATION

Corresponding Authors

angela.marinetti@cnrs.fr
xavier.guinchard@cnrs.fr

Notes

The authors declare no competing financial interests.

ACKNOWLEDGMENT

We thank the China Scholarship Council for PhD funding to Z. Z. and the CHARMMAT Labex (ANR-11-LABX0039) for the funding of V.S.

REFERENCES

- (a) Cera, G.; Bandini, M., Enantioselective Gold(I) Catalysis with Chiral Monodentate Ligands. *Isr. J. Chem.* **2013**, *53*, 848-855. (b) Zi, W.; Toste, D. F., Recent advances in enantioselective gold catalysis. *Chem. Soc. Rev.* **2016**, *45*, 4567-4589. (c) Li, Y.; Li, W.; Zhang, J., Gold-Catalyzed Enantioselective Annulations. *Chem. Eur. J.* **2017**, *23*, 467-512. (d) Mascareñas, J. L.; Varela, I.; López, F., Allenes and Derivatives in Gold(I)- and Platinum(II)-Catalyzed Formal Cycloadditions. *Acc. Chem. Res.* **2019**, *52*, 465-479.
- (a) Hamilton, G. L.; Kang, E. J.; Mba, M.; Toste, F. D., A Powerful Chiral Counterion Strategy for Asymmetric Transition Metal Catalysis. *Science* **2007**, *317*, 496-499. (b) LaLonde, R.; Wang, Z.; Mba, M.; Lackner, A.; Toste, F., Gold(I)-Catalyzed Enantioselective Synthesis of Pyrazolidines, Isoxazolidines, and Tetrahydrooxazines. *Angew. Chem. Int. Ed.* **2010**, *49*, 598-601. (c) Zi, W.; Toste, F. D., Gold(I)-Catalyzed Enantioselective Desymmetrization of 1,3-Diols through Intramolecular Hydroalkoxylation of Allenes. *Angew. Chem. Int. Ed.* **2015**, *54*, 14447-14451.
- (a) Aikawa, K.; Kojima, M.; Mikami, K., Axial Chirality Control of Gold(biphep) Complexes by Chiral Anions: Application to Asymmetric Catalysis. *Angew. Chem. Int. Ed.* **2009**, *48*, 6073-6077. (b) Aikawa, K.; Kojima, M.; Mikami, K., Synergistic Effect: Hydroalkoxylation of Allenes through Combination of Enantiopure BIPHEP-Gold Complexes and Chiral Anions. *Adv. Synth. Catal.* **2010**, *352*, 3131-3135. (c) Han, Z.-Y.; Guo, R.; Wang, P.-S.; Chen, D.-F.; Xiao, H.; Gong, L.-Z., Enantioselective concomitant creation of vicinal quaternary stereogenic centers via cyclization of alkynols triggered addition of azlactones. *Tetrahedron Lett.* **2011**, *52*, 5963-5967. (d) Tu, X.-F.; Gong, L.-Z., Highly Enantioselective Transfer Hydrogenation of Quinolines Catalyzed by Gold Phosphates: Achiral Ligand Tuning and Chiral-Anion Control of Stereoselectivity. *Angew. Chem. Int. Ed.* **2012**, *51*, 11346-11349. (e) Barreiro, E. M.; Brogini, D. F. D.; Adrio, L. A.; White, A. J. P.; Schwenk, R.; Togni, A.; Hii, K. K., Gold(I) Complexes of Conformationally Constricted Chiral Ferrocenyl Phosphines. *Organometallics* **2012**, *31*, 3745-3754. (f) Mourad, A. K.; Leutzow, J.; Czekelius, C., Anion-Induced Enantioselective Cyclization of DYNAMIDES to Pyrrolidines Catalyzed by Cationic Gold Complexes. *Angew. Chem. Int. Ed.* **2012**, *51*, 11149-11152. (g) Handa, S.; Lippincott, D. J.; Aue, D. H.; Lipshutz, B. H., Asymmetric Gold-Catalyzed Lactonizations in Water at Room Temperature. *Angew. Chem. Int. Ed.* **2014**, *53*, 10658-10662. (h) Shinde, V. S.; Mane, M. V.; Vanka, K.; Mallick, A.; Patil, N. T., Gold(I)/Chiral Brønsted Acid Catalyzed Enantioselective Hydroamination-Hydroarylation of Alkynes: The Effect of a Remote Hydroxyl Group on the Reactivity and Enantioselectivity. *Chem. Eur. J.* **2015**, *21*, 975-979. (i) Spittler, M.; Lutsenko, K.; Czekelius, C., Total Synthesis of (+)-Mesembrine Applying Asymmetric Gold Catalysis. *J. Org. Chem.* **2016**, *81*, 6100-6105. (j) Schiebl, J.; Schulmeister, J.; Doppia, A.; Wörner, E.; Rudolph, M.; Karch, R.; Hashmi, A. S. K., An Industrial Perspective on Counter Anions in Gold Catalysis: Underestimated with Respect to "Ligand Effects". *Adv. Synth. Catal.* **2018**, *360*, 2493-2502. (k) Miles, D. H.; Veguillas, M.; Toste, F. D., Gold(I)-catalyzed enantioselective bromocyclization reactions of allenenes. *Chem. Sci.* **2013**, *4*, 3427-3431.
- (a) Inamdar, S. M.; Konala, A.; Patil, N. T., When gold meets chiral Brønsted acid catalysts: extending the boundaries of enantioselective gold catalysis. *Chem. Commun.* **2014**, *50*, 15124-15135. (b) Jia, M.; Bandini, M., Counterion Effects in Homogeneous Gold Catalysis. *ACS Catal.* **2015**, *5*, 1638-1652.
- (a) Phipps, R. J.; Hamilton, G. L.; Toste, F. D., The progression of chiral anions from concepts to applications in asymmetric catalysis. *Nature Chem.* **2012**, *4*, 603-614. (b) Mahlau, M.; List, B., Asymmetric Counteranion-Directed Catalysis: Concept, Definition, and Applications. *Angew. Chem. Int. Ed.* **2013**, *52*, 518-533. (c) Brak, K.; Jacobsen, E. N., Asymmetric Ion-Pairing Catalysis. *Angew. Chem. Int. Ed.* **2013**, *52*, 534-561. (d) Parmar, D.; Sugiono, E.; Raja, S.; Rueping, M., Complete Field Guide to Asymmetric BINOL-Phosphate Derived Brønsted Acid and Metal Catalysis: History and Classification by Mode of Activation; Brønsted Acidity, Hydrogen Bonding, Ion Pairing, and Metal Phosphates. *Chem. Rev.* **2014**, *114*, 9047-9153.
- (a) Jiang, G.; List, B., Enantioselective hydrovinylation via asymmetric counteranion-directed ruthenium catalysis. *Chem. Commun.* **2011**, *47*, 10022-10024. (b) Barbazanges, M.; Augé, M.; Moussa, J.; Amouri, H.; Aubert, C.; Desmarests, C.; Fensterbank, L.; Gandon, V.; Malacria, M.; Ollivier, C., Enantioselective Ir(I)-Catalyzed Carbocyclization of 1,6-Enynes by the Chiral Counterion Strategy. *Chem. Eur. J.* **2011**, *17*, 13789-13794. (c) Augé, M.; Barbazanges, M.; Tran, A. T.; Simonneau, A.; Elley, P.; Amouri, H.; Aubert, C.; Fensterbank, L.; Gandon, V.; Malacria, M.; Moussa, J.; Ollivier, C., Atroposelective [2+2+2] cycloadditions catalyzed by a rhodium(I)-chiral phosphate system. *Chem. Commun.* **2013**, *49*, 7833-7835. (d) Augé, M.; Feraldi-Xypolia, A.; Barbazanges, M.; Aubert, C.; Fensterbank, L.; Gandon, V.; Kolodziej, E.; Ollivier, C., Double-Stereodifferentiation in Rhodium-Catalyzed [2 + 2 + 2] Cycloaddition: Chiral Ligand/Chiral Counterion Matched Pair. *Org. Lett.* **2015**, *17*, 3754-3757. (e) Barbazanges, M.; Caytan, E.; Lesage, D.; Aubert, C.; Fensterbank, L.; Gandon, V.; Ollivier, C., Chiral Phosphate in Rhodium-Catalyzed Asymmetric [2+2+2] Cycloaddition: Ligand, Counterion, or Both? *Chem. Eur. J.* **2016**, *22*, 8553-8558. (f) Mukherjee, S.; List, B., Chiral counteranions in asymmetric transition-metal catalysis: Highly enantioselective Pd/Bronsted acid-catalyzed direct alpha-allylation of aldehydes. *J. Am. Chem. Soc.* **2007**, *129*, 11336-11337. (g) Llewellyn, D. B.; Adamson, D.; Arndtsen, B. A., A Novel Example of Chiral Counteranion Induced Enantioselective Metal Catalysis: The Importance of Ion-Pairing in Copper-Catalyzed Olefin Aziridination and Cyclopropanation. *Org. Lett.* **2000**, *2*, 4165-4168.
- (a) Yao, T.; Zhang, X.; Larock, R. C., Synthesis of Highly Substituted Furans by the Electrophile-Induced Coupling of 2-(1-Alkynyl)-2-alken-1-ones and Nucleophiles. *J. Org. Chem.* **2005**, *70*, 7679-7685. (b) Yao, T. L.; Zhang, X. X.; Larock, R. C., AuCl₃-catalyzed synthesis of highly substituted furans from 2-(1-alkynyl)-2-alken-1-ones. *J. Am. Chem. Soc.* **2004**, *126*, 11164-11165.
- (a) Iwai, T.; Akiyama, Y.; Tsunoda, K.; Sawamura, M., Synthesis and structures of a chiral phosphine-phosphoric acid ligand and its rhodium(I) complexes. *Tetrahedron: Asymmetry* **2015**, *26*, 1245-1250. (b) Nakamura, A.; Anselment, T. M. J.; Claverie, J.; Goodall, B.; Jordan, R. F.; Mecking, S.; Rieger, B.; Sen, A.; van Leeuwen, P. W. N. M.; Nozaki, K., Ortho-Phosphinobenzenesulfonate: A Superb Ligand for Palladium-Catalyzed Coordination-Insertion Copolymerization of Polar Vinyl

- Monomers. *Acc. Chem. Res.* **2013**, *46*, 1438-1449. (c) Brown, M. K.; May, T. L.; Baxter, C. A.; Hoveyda, A. H., All-Carbon Quaternary Stereogenic Centers by Enantioselective Cu-Catalyzed Conjugate Additions Promoted by a Chiral N-Heterocyclic Carbene. *Angew. Chem. Int. Ed.* **2007**, *46*, 1097-1100.
9. (a) Zhang, Z.-M.; Chen, P.; Li, W.; Niu, Y.; Zhao, X.-L.; Zhang, J., A New Type of Chiral Sulfinamide Monophosphine Ligands: Stereodivergent Synthesis and Application in Enantioselective Gold(I)-Catalyzed Cycloaddition Reactions. *Angew. Chem. Int. Ed.* **2014**, *53*, 4350-4354. (b) Wang, Z.; Nicolini, C.; Hervieu, C.; Wong, Y.-F.; Zannoni, G.; Zhang, L., Remote Cooperative Group Strategy Enables Ligands for Accelerative Asymmetric Gold Catalysis. *J. Am. Chem. Soc.* **2017**, *139*, 16064-16067.
10. Recent examples of chiral bifunctional Au(I) complexes include: (a) Zuccarello, G.; Mayans, J. G.; Escofet, I.; Scharnagel, D.; Kirillova, M. S.; Pérez-Jimeno, A. H.; Calleja, P.; Boothe, J. R.; Echavarren, A. M., Enantioselective Folding of Enynes by Gold(I) Catalysts with a Remote C2-Chiral Element. *J. Am. Chem. Soc.* **2019**, *141*, 11858-11863. (b) Wang, Z.; Nicolini, C.; Hervieu, C.; Wong, Y.-F.; Zannoni, G.; Zhang, L., Remote Cooperative Group Strategy Enables Ligands for Accelerative Asymmetric Gold Catalysis. *J. Am. Chem. Soc.* **2017**, *139*, 16064-16067. (c) Li, T.; Zhang, L., Bifunctional Biphenyl-2-ylphosphine Ligand Enables Tandem Gold-Catalyzed Propargylation of Aldehyde and Unexpected Cycloisomerization. *J. Am. Chem. Soc.* **2018**, *140*, 17439-17443. (d) Zhang, J.-Q.; Liu, Y.; Wang, X.-W.; Zhang, L., Synthesis of Chiral Bifunctional NHC Ligands and Survey of Their Utilities in Asymmetric Gold Catalysis. *Organometallics* **2019**, *38*, 3931-3938.
11. (a) Hatano, M.; Ishihara, H.; Goto, Y.; Ishihara, K., Remote Tris(pentafluorophenyl)borane-Assisted Chiral Phosphoric Acid Catalysts for the Enantioselective Diels-Alder Reaction. *Synlett* **2016**, *27*, 564 - 570. (b) Ma, J.; Kass, S. R., Asymmetric Arylation of 2,2,2-Trifluoroacetophenones Catalyzed by Chiral Electrostatically-Enhanced Phosphoric Acids. *Org. Lett.* **2018**, *20*, 2689 - 2692. (c) Tang, H.-Y.; Lu, A.-D.; Zhou, Z.-H.; Zhao, G.-F.; He, L.-N.; Tang, C.-C., Chiral Phosphoric Acid Catalyzed Asymmetric Friedel-Crafts Alkylation of Indoles with Simple α,β -Unsaturated Aromatic Ketones. *Eur. J. Org. Chem.* **2008**, 1406-1410. (d) Tang, H.-Y.; Zhang, Z.-B., Chiral phosphoric acid catalyzed asymmetric friedel-crafts alkylation of indoles with nitroolefins. *Phosphorus, Sulfur and Silicon and the Related Elements* **2011**, *186*, 2038 - 2046. (e) Yao, Y.; Shu, H.; Tang, B.; Chen, S.; Lu, Z.; Xue, W., Synthesis, characterization and application of some axially chiral binaphthyl phosphoric acids in asymmetric mannich reaction. *Chinese Journal of Chemistry* **2015**, *33*, 601 - 609.
12. Matsui, K.; Takizawa, S.; Sasai, H., A Brønsted Acid and Lewis Base Organocatalyst for the Aza-Morita-Baylis-Hillman Reaction. *Synlett* **2006**, *2006*, 0761-0765.
13. Zhang, X.-N.; Shi, M., A Highly Nucleophilic Multifunctional Chiral Phosphane-Catalyzed Asymmetric Intramolecular Rauhut-Currrier Reaction. *Eur. J. Org. Chem.* **2012**, *2012*, 6271-6279.
14. Xu, M.-H.; Pu, L., A New 1,1'-Binaphthyl-Based Catalyst for the Enantioselective Phenylacetylene Addition to Aromatic Aldehydes without Using a Titanium Complex. *Org. Lett.* **2002**, *4*, 4555-4557.
15. See the Supporting Information for details.
16. Building of polymeric chains from (S)-6 can not be ruled out at this stage.
17. Raducan, M.; Moreno, M.; Bour, C.; Echavarren, A. M., Phosphate ligands in the gold(I)-catalysed activation of enynes. *Chem. Commun.* **2012**, *48*, 52-54.
18. Echavarren showed that phosphine-gold-phosphate present a 31P-31P coupling constant of about 2.4-3.9 Hz. See ref. x
19. (a) Liu, S.; Yang, P.; Peng, S.; Zhu, C.; Cao, S.; Li, J.; Sun, J., Gold-catalyzed sequential annulations towards 3,4-fused bi/tri-cyclic furans involving a [3+2+2] cycloaddition. *Chem. Commun.* **2017**, *53*, 1152-1155. (b) Zheng, Y.; Chi, Y.; Bao, M.; Qiu, L.; Xu, X., Gold-Catalyzed Tandem Dual Heterocyclization of Enynones with 1,3,5-Triazines: Bicyclic Furan Synthesis and Mechanistic Insights. *J. Org. Chem.* **2017**, *82*, 2129-2135.
20. Wang, Y.; Zhang, P.; Qian, D.; Zhang, J., Highly Regio-, Diastereo-, and Enantioselective Gold(I)-Catalyzed Intermolecular Annulations with N-Allenamides at the Proximal C=C Bond. *Angew. Chem. Int. Ed.* **2015**, *54*, 14849-14852.
21. Wang, Y.; Zhang, Z.-M.; Liu, F.; He, Y.; Zhang, J., Ming-Phos/Gold(I)-Catalyzed Diastereo- and Enantioselective Synthesis of Indolyl-Substituted Cyclopenta[c]furans. *Org. Lett.* **2018**, *20*, 6403-6406.
22. Liu, F.; Yu, Y.; Zhang, J., Highly Substituted Furo[3,4-d][1,2]oxazines: Gold-Catalyzed Regiospecific and Diastereoselective 1,3-Dipolar Cycloaddition of 2-(1-Alkynyl)-2-alken-1-ones with Nitrones. *Angew. Chem. Int. Ed.* **2009**, *48*, 5505-5508.
23. (a) Liu, X.; Pan, Z.; Shu, X.; Duan, X.; Liang, Y., Bu₄N AuCl₄-catalyzed synthesis of highly substituted furans from 2-(1-alkynyl)-2-alken-1-ones in ionic liquids: An air-stable and recyclable catalytic system. *Synlett* **2006**, 1962-1964. (b) Qi, J.; Teng, Q.; Thirupathi, N.; Tung, C.-H.; Xu, Z., Diastereoselective Synthesis of Polysubstituted Spirocyclopenta[c]furans by Gold-Catalyzed Cascade Reaction. *Org. Lett.* **2019**, *21*, 692-695.
24. Oh, C. H.; Reddy, V. R.; Kim, A.; Rhim, C. Y., Nucleophile-assisted Pt-catalyzed cyclization of enynes: an access to synthesis of highly substituted furans. *Tetrahedron Lett.* **2006**, *47*, 5307-5310.
25. (a) Xiao, Y.; Zhang, J., Tetrasubstituted furans by a Pd(II)-catalyzed three-component Michael addition/cyclization/cross-coupling reaction. *Angew. Chem. Int. Ed.* **2008**, *47*, 1903-1906. (b) Liu, R.; Zhang, J., Tetrasubstituted Furans by Pd-II-Catalyzed Three-Component Domino Reactions of 2-(1-Alkynyl)-2-alken-1-ones with Nucleophiles and Vinyl Ketones or Acrolein. *Chem. Eur. J.* **2009**, *15*, 9303-9306. (c) Xiao, Y.; Zhang, J., Palladium(II)-Catalyzed Domino Reaction of 2-(1-Alkynyl)-2-alken-1-ones with Nucleophiles: Scope, Mechanism and Synthetic Application in the Synthesis of 3,4-Fused Bicyclic Tetrasubstituted Furans. *Adv. Synth. Catal.* **2009**, *351*, 617-629. (d) Li, W.; Zhang, J., Tetrasubstituted furans by Pd(II)/Cu(I) cocatalyzed three-component domino reactions of 2-(1-alkynyl)-2-alken-1-ones, nucleophiles and diaryliodonium salts. *Chem. Commun.* **2010**, *46*, 8839-8841.
26. Force, G.; Ki, Y. L. T.; Isaac, K.; Retailleau, P.; Marinetti, A.; Betzer, J. F., Paracyclophane-based Silver Phosphates as Catalysts for Enantioselective Cycloisomerization/Addition Reactions: Synthesis of Bicyclic Furans. *Adv. Synth. Catal.* **2018**, *360*, 3356-3366.
27. (a) Patil, N. T.; Wu, H. Y.; Yamamoto, Y., Cu(I) catalyst in DMF: An efficient catalytic system for the synthesis of furans from 2-(1-alkynyl)-2-alken-1-ones. *J. Org. Chem.* **2005**, *70*, 4531-4534. (b) Rauniyar, V.; Wang, Z. J.; Burks, H. E.; Toste, F. D., Enantioselective Synthesis of Highly Substituted Furans by a Copper(II)-Catalyzed Cycloisomerization-Indole Addition Reaction. *J. Am. Chem. Soc.* **2011**, *133*, 8486-8489. (c) Huang, L.; Hu, F.; Ma, Q.; Hu, Y., CuBr-catalyzed cascade reaction of 2-substituted-3-(1-alkynyl)chromones to synthesize functionalized 3-acylfurans. *Tetrahedron Lett.* **2013**, *54*, 3410-3414.
28. Pathipati, S. R.; van der Werf, A.; Eriksson, L.; Selander, N., Diastereoselective Synthesis of Cyclopenta[c]furans by a Catalytic Multicomponent Reaction. *Angew. Chem. Int. Ed.* **2016**, *55*, 11863-11866.
29. Liu, F.; Qian, D.; Li, L.; Zhao, X.; Zhang, J., Diastereo- and Enantioselective Gold(I)-Catalyzed Intermolecular Tandem Cyclization/3+3 Cycloadditions of 2-(1-Alkynyl)-2-alken-1-ones with Nitrones. *Angew. Chem. Int. Ed.* **2010**, *49*, 6669-6672.
30. The complex isolated by evaporation of the solvents, after the NMR experiments in Scheme 3, displays somewhat lower catalytic activity and enantioselectivity with respect to the in situ generated catalyst. See the Supporting Information for details.
31. Carvajal, M. A.; Novoa, J. J.; Alvarez, S., Choice of Coordination Number in d10 Complexes of Group 11 Metals. *J. Am. Chem. Soc.* **2004**, *126*, 1465-1477.
32. Catalysts 7a,b and 11a,b were generated by reaction with the corresponding silver salts, filtrated, checked by 31P NMR and used as solutions. See the Supporting Information.
33. (a) Wang, D.; Cai, R.; Sharma, S.; Jirak, J.; Thummanapelli, S. K.; Akhmedov, N. G.; Zhang, H.; Liu, X.; Petersen, J. L.; Shi, X., "Silver Effect" in Gold(I) Catalysis: An Overlooked Important Factor. *J. Am. Chem. Soc.* **2012**, *134*, 9012-9019. (b) Weber, D.; Gagné, M. R., Dinuclear Gold-Silver

- Resting States May Explain Silver Effects in Gold(I)-Catalysis. *Org. Lett.* **2009**, *11*, 4962-4965. (c) Han, J.; Shimizu, N.; Lu, Z.; Amii, H.; Hammond, G. B.; Xu, B., Efficient Generation and Increased Reactivity in Cationic Gold via Brønsted Acid or Lewis Acid Assisted Activation of an Imidogold Precatalyst. *Org. Lett.* **2014**, *16*, 3500-3503. (d) Zhdanko, A.; Maier, M. E., Explanation of "Silver Effects" in Gold(I)-Catalyzed Hydroalkoxylation of Alkynes. *ACS Catal.* **2015**, *5*, 5994-6004. (e) Homs, A.; Escofet, I.; Echavarren, A. M., On the Silver Effect and the Formation of Chloride-Bridged Digold Complexes. *Org. Lett.* **2013**, *15*, 5782-5785.
34. (a) Wang, W.; Hammond, G. B.; Xu, B., Ligand Effects and Ligand Design in Homogeneous Gold(I) Catalysis. *J. Am. Chem. Soc.* **2012**, *134*, 5697-5705. (b) Ranieri, B.; Escofet, I.; Echavarren, A. M., Anatomy of gold catalysts: facts and myths. *Org. Biomol. Chem.* **2015**, *13*, 7103-7118. (c) Schmidbaur, H.; Schier, A., Silver-free Gold(I) Catalysts for Organic Transformations. *Zeitschrift Fur Naturforschung Section B-a Journal of Chemical Sciences* **2011**, *66*, 329-350.
35. Teles, J. H.; Brode, S.; Chabanas, M., Cationic Gold(I) Complexes: Highly Efficient Catalysts for the Addition of Alcohols to Alkynes. *Angew. Chem. Int. Ed.* **1998**, *37*, 1415-1418.
36. Gaillard, S.; Bosson, J.; Ramón, R. S.; Nun, P.; Slawin, A. M. Z.; Nolan, S. P., Development of Versatile and Silver-Free Protocols for Gold(I) Catalysis. *Chem. Eur. J.* **2010**, *16*, 13729-13740.
37. Lavallo, V.; Frey, G. D.; Kousar, S.; Donnadieu, B.; Bertrand, G., Allene formation by gold catalyzed cross-coupling of masked carbenes and vinylidenes. *Proc. Natl. Acad. Sci.* **2007**, *104*, 13569-13573.
38. (a) Guérinot, A.; Fang, W.; Sircoglou, M.; Bour, C.; Bezenine-Lafollée, S.; Gandon, V., Copper Salts as Additives in Gold(I)-Catalyzed Reactions. *Angew. Chem. Int. Ed.* **2013**, *52*, 5848-5852. (b) Fang, W.; Passet, M.; Guérinot, A.; Bour, C.; Bezenine-Lafollée, S.; Gandon, V., Silver-Free Two-Component Approach in Gold Catalysis: Activation of [LAuCl] Complexes with Derivatives of Copper, Zinc, Indium, Bismuth, and Other Lewis Acids. *Chem. Eur. J.* **2014**, *20*, 5439-5446.
39. Li, F.; Wang, N.; Lu, L.; Zhu, G., Regioselective Hydration of Terminal Alkynes Catalyzed by a Neutral Gold(I) Complex [(IPr)AuCl] and One-Pot Synthesis of Optically Active Secondary Alcohols from Terminal Alkynes by the Combination of [(IPr)AuCl] and Cp*RhCl[(R,R)-TsDPEN]. *J. Org. Chem.* **2015**, *80*, 3538-3546.

• **Asymmetric Au(I)
catalysis**

